EPR of S-state ions in aragonite $CaCO_3$ and cerussite $PbCO_3$

1989 J. Phys.: Condens. Matter 1 5481

(http://iopscience.iop.org/0953-8984/1/32/017)

J. Phys.: Condens. Matter **1** (1989) 5481–5487. Printed in the UK

EPR of S-state ions in aragonite $CaCO_3$ and cerussite $PbCO_3$

F Prissok and G Lehmann

Institut für Physikalische Chemie, Westfalische Wilhelms-Universität, D-4400 Münster, Federal Republic of Germany

Received 20 January 1989

Abstract. EPR measurements on single crystals of natural aragonite ($CaCo_3$) and cerussite ($PbCO_3$) revealed the presence of Gd^{3+} in both and of a small amount of Eu^{2+} in the latter mineral. Their zero-field and hyperfine splitting parameters were determined at room temperature. The site symmetry of Gd^{3+} in aragonite is lowered, this being most likely due to local charge compensation. The zero-field splitting patterns in cerussite can, within the limits of error of the crystal structure data, be perfectly reproduced by the distortion of the Pb host site as shown by application of the superposition model. Slight deviations are observed for Gd^{3+} in aragonite and very pronounced ones for Mn^{2+}, for which EPR results from the literature were evaluated. For Gd^{3+} this may be due to the presence of a charge compensator, whereas for Mn^{2+} local relaxations as a result of the size mismatch between host and impurity ion must result in much larger distortions.

1. Introduction

The anhydrous carbonates of divalent metal ions crystallise in two types of structures: the calcite structure with space group $D_{3d}^6(R\bar{3}c)$ for the smaller ions (Effenberger *et al* 1981) and the aragonite structure with space group $D_{2h}^{16}(Pnma)$ for the larger ones (de Villiers 1971, Sahl 1974). $CaCO_3$ takes an intermediate position since it occurs naturally in both modifications with the calcite structure as the stable modification under normal temperature and pressure conditions, and in fact the names of these structural families are taken from the minerals of this compound.

Whereas the divalent ions in the calcite structure are sixfold coordinated with a trigonal site symmetry, their coordination number is 9 in the aragonite structure with point symmetry C_s since they are located in the mirror plane perpendicular to the crystal *b* axis. This must therefore be a principal axis of the EPR spectra of impurity ions in unperturbed cation sites. EPR data were reported for Mn^{2+} in aragonite (Ślezak *et al* 1979, Lech *et al* 1984), and indeed the earlier single-crystal study confirmed this expectation and also demonstrated the presence of this ion in two magnetically non-equivalent sites.

The f^7 ions Gd^{3+} and Eu^{2+} are equally well detectable by EPR at normal temperatures, and according to their ionic radii (Shannon and Prewitt 1969) they should substitute for both Ca and Pb. Indeed in a survey of natural specimens from different locations we detected them in one specimen each in sufficient quantities for detailed evaluation of their spin-Hamiltonian parameters for zero-field (ZFS) and hyperfine splitting. The

0953-8984/89/325481 + 07 $02.50

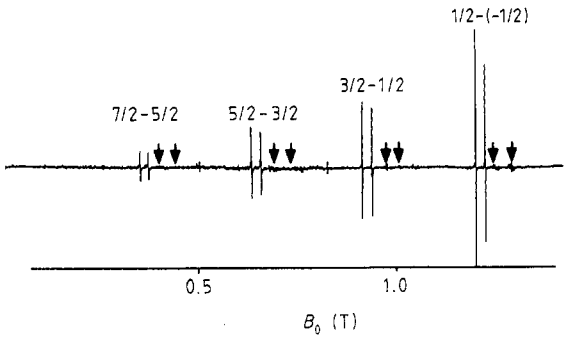

Figure 1. EPR spectrum of Gd^{3+} and Eu^{2+} in cerussite at 33.5 GHz and room temperature for the magnetic field perpendicular to *b* and 6° from *a*. The weak multiplets due to Eu^{2+} are marked by arrows.

former data were subjected to a superposition-model (SPM) analysis (Newman and Urban 1972, 1975); data for Mn^{2+} in aragonite from the literature were evaluated in the same way, although the size mismatch of host and impurity ion was expected to cause significant local relaxations as in the cases of Fe^{3+} and Cr^{3+} in Al sites (Büscher *et al* 1987).

2. Experimental procedure

Single crystals of aragonite from Horschenz and of cerussite from Mies, both in Bohemia, Czechoslovakia, were investigated by EPR at X- and Q-band frequencies using commercial spectrometers of Bruker Analytische Messtechnik GmbH, Karlsruhe. The computer program used for evaluation of the spin-Hamiltonian parameters is described elsewhere (Behner and Lehmann 1987). A program for simulation of rotational diagrams including the fine structure parameters additionally required for low site symmetries has been recently developed. For superposition analysis of the crystal structure data a computer program suitable for monoclinic or higher point-symmetries (Büscher 1985) was used.

3. Results and discussion

3.1. Cerussite

The EPR spectra were recorded at Q-band frequencies for rotations around all three crystal axes. The concentration of Gd^{3+} was about seven times higher than that of Eu^{2+}, and consequently the transitions of lower intensity for the latter are not clearly visible in the spectrum reproduced in figure 1. Weak hyperfine satellites were observed for Gd^{3+}. If they are assigned to the outer hyperfine satellites of the $^{155,157}Gd$ nuclei with $I = \frac{3}{2}$, a value of $A = 22$ MHz is obtained. It is rather high compared with, e.g. a value of 15 MHz for this ion in $SrCl_2$ (van Ormondt *et al* 1980). For Eu^{2+} hyperfine splittings of 96 and 42 MHz for the ^{151}Eu and ^{153}Eu isotopes were observed, in good agreement with other data (e.g. of -98 MHz for ^{151}Eu in CaF_2 (Hurren *et al* 1969)). An example of this hyperfine structure is shown in figure 2. The fine structure parameters for these

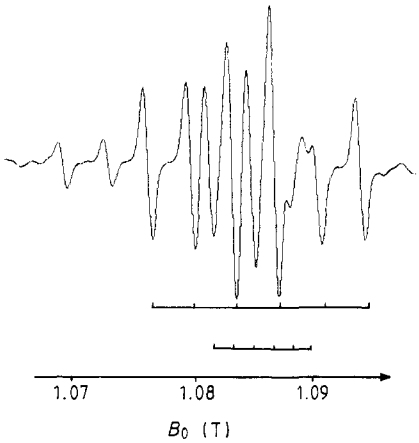

Figure 2. Enlarged portion of the EPR spectrum of figure 1 showing the two hyperfine multiplets of ^{151}Eu and ^{155}Eu for the 3/2–1/2 transition. The additional weaker signals are due to forbidden transitions of Gd^{3+}.

Table 1. Spin Hamiltonian parameters for Gd^{3+} and Eu^{2+} in aragonite and cerussite. All b_n^m are in cm^{-1}; the signs of b_2^0 and b_2^2 are predicted by the results of the superposition analysis (see text).

	Aragonite	Cerussite	
Parameter	Gd^{3+}	Gd^{3+}	Eu^{2+}
b_2^0	−0.123(1)	0.132(1)	0.133(1)
b_2^2	−0.087(5)	0.04475(4)	0.008(1)
b_4^0	+0.036(10)	0.0004(2)	0.000054(10)
b_4^2	+0.007(2)	−0.010(4)	0.00056(16)
b_4^3	−0.028(20)	0.14(8)	−0.16(1)
b_4^4	−0.0038(10)	−0.008(2)	−0.0048(10)

ions are listed in table 1 and the directions of their principal axes in table 2. The signs of the second order ZFS parameters could not be determined absolutely, but the results of the SPM analyses lead to clear predictions for them, as will be shown below. The parameter b_4^3 and its limits of error are rather large for both ions.

No sign for a local charge compensation of the extra positive charge of Gd^{3+} was detectable. It must either occur randomly in the lattice or by exchange of a Ca^{2+} in the mirror plane by a monovalent cation like Na^+ or K^+, thus retaining the monoclinic site symmetry.

In the SPM analyses we compare the distortions obtained from the second-order ZFS parameters and the positions of their principal axes with those obtained from the crystal structure refinement for cerussite (Sahl 1974) in the same manner as described in previous works (e.g. Heming and Lehmann 1987). For the crystal structure data (broken curves in figures 3, 5–7 later) these distortions are given by

$$d_c = \tfrac{1}{2} \sum_i (3\cos^2\theta_i - 1)(R_0/R_i)^{t_2} \tag{1}$$

where the summation runs over all ligands $i = 1$ to 9 for the MO_9 units and θ_i are the angles between the M–O_i directions and the direction considered. An exponent $t_2 = 2$

Table 2. Direction cosines of the magnetic axes systems with respect to the crystallographic one.

Mineral	Impurity	Magnetic axis	Crystallographic axes		
			a	*b*	*c*
Aragonite	Gd^{3+}	*x*	−0.529	−0.044	0.847
		y	0.848	−0.028	0.529
		z	0.000	0.998	0.052
Cerussite	Gd^{3+}	*x*	0.309	0.000	−0.951
		y	0.000	1.000	0.000
		z	0.951	0.000	0.309
	Eu^{2+}	*x*	0.000	1.000	0.000
		y	−0.407	0.000	0.914
		z	0.914	0.000	0.407

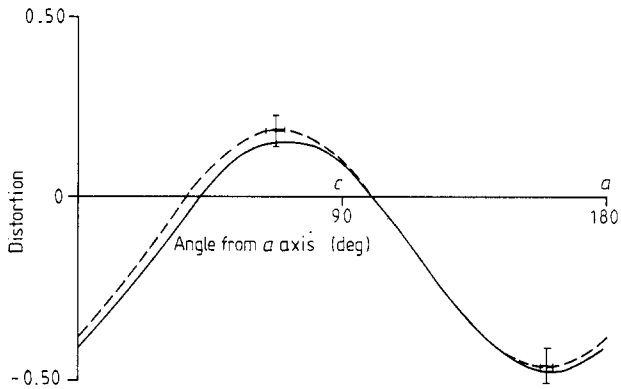

Figure 3. Comparison of the distortions d_s from EPR (full curve) and d_c from crystal structure data (broken curve) with limits of error indicated by bars for Gd^{3+} in cerussite in the *ac* plane.

was chosen for both Gd^{3+} and Eu^{2+}, and the reference distance R_0 was chosen as the normal M–O bond distance in pure compounds of these paramagnetic ions, namely 242 pm and 252 pm for Gd^{3+} and Eu^{2+}, respectively.

The distortions obtained from the ZFS data are given by

$$d_s = (1/2\bar{b}_2)[(3\cos^2\vartheta - 1)b_2^0 + \sin^2\vartheta\cos^2\varphi(b_2^2)] \tag{2}$$

where the angles ϑ and φ define the direction within the principal axes system of the ZFS tensor. The value of the intrinsic ZFS parameter $\bar{b}_2$ depends on the choice of both t_2 and R_0 and is chosen to match the distortions along the *z* axis for both d_c and d_s (in the cases where good overall agreement is obtained). As is evident from figures 3 and 4, the agreement for the whole patterns is perfect within the limits of error of the crystal structure data marked by bars in these figures, with very similar values of $\bar{b}_2$ of $-0.28\ cm^{-1}$ and $-0.26\ cm^{-1}$ for Gd^{3+} and Eu^{2+}, respectively. Since negative values of these intrinsic ZFS parameters were observed in previous cases (Newman and Urban 1972, Vishwamittar and Puri 1974), positive signs are predicted for b_2^0 and b_2^2. The values of $\bar{b}_2$ are two to three times higher than obtained for other systems in these previous

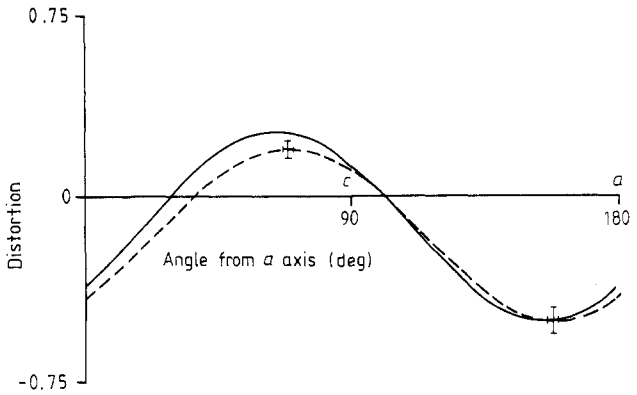

Figure 4. Comparison of distortions d_s and d_c for Eu^{2+} in cerussite.

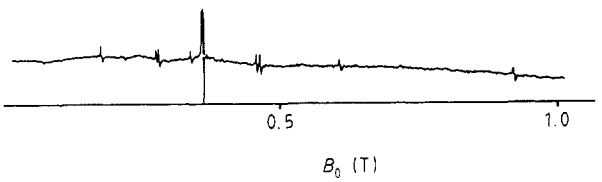

Figure 5. EPR spectrum of Gd^{3+} in aragonite at 9.5 GHz and room temperature for the magnetic field perpendicular to the *b* axis and 32° from *c*. A splitting into two signals due to triclinic site symmetry is clearly visible for some transitions. The most intense signal near $g = 2$ is due to a radiation defect.

investigations. As in other cases (Newman 1971, Newman and Urban 1975, Kuriata *et al* 1982, Amoretti *et al* 1982, 1984) the low value of the exponent t_2 can be assumed to result from two opposing terms of similar size with much higher, but slightly different exponents.

3.2. *Aragonite*

The spectra of Gd^{3+} were measured for rotations around the crystal *a* and *b* axes at X- and Q-band frequencies. Figure 5 shows a spectrum for the magnetic field perpendicular to *b* and 32° from *c*. A slight splitting into magnetically non-equivalent sites indicative of a lowering of the site symmetry to triclinic is apparent for some transitions. No hyperfine satellites could be resolved in this case. The ZFS parameters determined from the rotational diagrams are also listed in table 1, and the directions of the principal axes are given in table 2. As in cerussite, the *g*-factors were assumed as isotropic and equal to the free-electron value, a reasonable approximation for these S-state ions.

The lowering of the site symmetry is most likely due to local charge compensation. Exchange of a CO_3^{2-} with a BO_3^{3-} (or PO_3^{3-}) group is in our view the most likely mechanism since exchange of a more distant Ca^{2+} outside the mirror plane of the Gd^{3+} is energetically less favourable.

The SPM analysis for this system with the same values of R_0, t_2 and $\bar{b}_2$ as in cerussite predicts a negative sign of b_2^0 and b_2^2. As shown in figure 6, the principal axes again agree within the experimental error of $\pm 1.2°$, but larger differences in the absolute values are observed for the *x* axis which also cause an interchange between *y* and *z* for both curves; Whereas experimentally the *z* axis is found to (almost) coincide with the *b* axis, the crystal structure data predict it to lie in the *ac* plane at 159°, the position of the *y* axis of

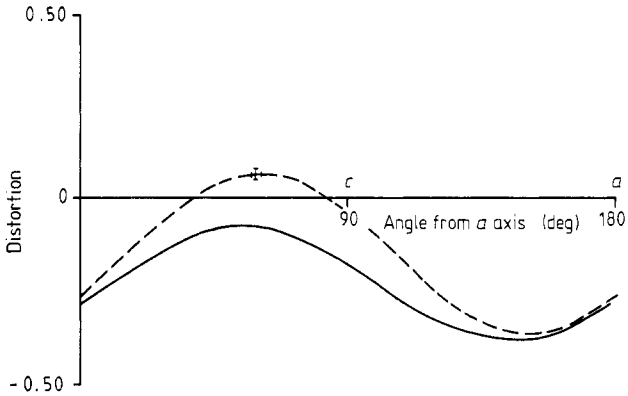

Figure 6. Comparison of distortions d_s and d_c for Gd^{3+} in aragonite.

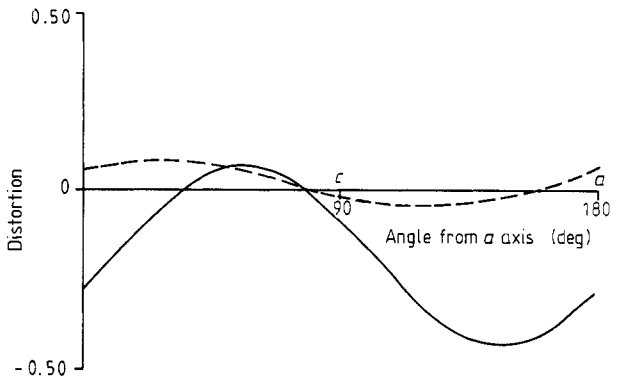

Figure 7. Comparison of distortions d_s and d_c for Mn^{2+} in aragonite.

the ZFS tensor. These differences may well be caused by changes in the local geometry of the oxygen neighbours due to local charge compensation. In view of the still disputed applicability of the SPM for f^7 ions (e.g. den Hartog and Bijvank 1978), however, the agreement for these ions in both cerussite and aragonite is remarkable.

The ZFS data for Mn^{2+} in aragonite from the literature (Ślezak *et al* 1979, Lech *et al* 1984) were subjected to the same superposition analysis. In this case a value of $t_2 = 7$ was obtained experimentally (Newman and Siegel 1976, Siegel and Müller 1979, Heming *et al* 1981) and published values of $R_0 = 220$ pm and $\bar{b}_2 = -0.05\ cm^{-1}$ (Heming and Lehmann, 1987) were used. The data in figure 7 again indicate considerable discrepancies in the positions of the extreme values and still more pronounced ones in the magnitudes of the ZFS data. The cause of these large discrepancies can only be a considerable local relaxation resulting from the size mismatch between Mn^{2+} and the host ion Ca^{2+}. A considerable change of the trigonal angle was also observed for Mn^{2+} in dolomite (Prissok and Lehmann 1986). For Gd^{3+} in aragonite such local relaxations should not be of importance since its size matches that of Ca^{2+} quite closely (Shannon and Prewitt 1969). On the other hand, in view of the larger size of Pb^{2+} the excellent agreement for cerussite is even more remarkable.

For Gd^{3+} in calcite (Atsarkin *et al* 1965, Marshall and Serway 1968) a value of $\bar{b}_2 = -0.16\ cm^{-1}$ is obtained with $t_2 = 2$. When compared with that in the aragonite

structures, it suggests a smaller deviation of the trigonal angle from the ideal value than that observed in the pure compound. But this value of the intrinsic ZFS parameter is well within the range observed for other systems with oxygen as ligand, and in any case an isolated system in axial site symmetry does not allow a critical validity test of the SPM since the directions of the principal axes are completely fixed by symmetry.

Acknowledgment

This work was supported by grants from the Deutsche Forschungsgemeinschaft.

References

Amoretti G, Calestani G and Giori D C 1984 *Z. Naturf.* **39** a, 778–82
Amoretti G, Fava C and Varacca V 1982 *Z. Naturf.* **37** a 536–45
Atsarkin V A, Lushnikov V G and Sorokina L P 1965 *Sov. Phys.–Solid State* **7** 1912–4
Behner S and Lehmann G 1987 *J. Phys. Chem Solids* **48** 555–8
Büscher R 1985 *Dissertation* Westfalische Wilhelms-Universität, Münster
Büscher R, Such K P and Lehmann G 1987 *Phys. Chem. Miner.* **14** 553–9
den Hartog H W and Bijvank E 1978 *J. Phys. C: Solid State Phys.* **11** L33–5
de Villiers J P R 1971 *Am. Mineral.* **56** 759–67
Effenberger M, Mereiter K and Zemann J 1981 *Z. Kristallogr.* **156** 233–43
Heming M and Lehmann G 1987 *Electronic Magnetic Resonance of the Solid State* ed. J A Weil (Ottawa: Canadian Society for Chemistry) p 163–74
Heming M, Lehmann G, Henkel G and Krebs B 1981 *Z. Naturf.* **36** a 286–93
Hurren W R, Nelson H M, Larson E G and Gardner J H 1969 *Phys. Rev.* **185** 624–9
Kuriata J, Guskos N and Rewaj T 1982 *Acta Phys. Polon.* A **62** 199–206
Lech S, Ślezak A and Bósko I 1984 *Phys. Status Solidi* b **126** 371–80
Marshall S A and Serway R A 1968 *Phys. Rev.* **171** 345–9
Newman D J 1971 *Adv. Phys.* **20** 197–256
Newman D J and Siegel E 1976 *J. Phys. C: Solid State Phys.* **9** 4285–92
Newman D J and Urban W 1972 *J. Phys. C: Solid State Phys.* **5** 3101–9
—— 1975 *Adv. Phys.* **24** 793–844
Prissok F and Lehmann G 1986 *Phys. Chem. Miner.* **13** 331–6
Sahl K 1974 *Z. Kristallogr.* **139** 215–22
Shannon R D and Prewitt C T 1969 *Acta Crystallogr.* B **25** 925–46
Siegel E and Müller K A 1979 *Phys. Rev.* B **19** 109–20
Ślezak A, Lech S and Bósko I 1979 *Phys. Status Solidi* a **54** 755–9
van Ormondt D, Reddy K V and van Ast M A 1980 *J. Magn. Reson.* **37** 195–204
Vishwamittar and Puri J P 1974 *J. Chem. Phys.* **61** 3720–7